

RNAi as a tool to inhibit the angiogenic potential of human Mesenchymal Stem/Stromal Cells in malignancy

Cristiana Ulpiano *, Master in Biotechnology, *Instituto Superior Técnico – Lisboa*

*Stem Cell Engineering Research Group & Bioengineering Research Group, iBB – Institute for Bioengineering and Biosciences, Instituto Superior Técnico
cristiana.ulpiano@tecnico.ulisboa.pt

ABSTRACT

Mesenchymal Stem/Stromal Cells (MSCs) have an active role in supporting the maintenance of a dynamic and homeostatic tissue microenvironment by secretion of a broad range of biologically active molecules. Upon interaction with cancer cells, MSCs become active participants in tumour development namely by promoting angiogenesis through the secretion of pro-angiogenic molecules, such as vascular endothelial growth factor (VEGF). Considering that tumour angiogenesis is one of the hallmarks of cancer progression, blocking VEGF production by the cells present in tumour microenvironment, might represent a potential approach to slow down tumour growth. In this context, RNA interference-mediated silencing appears a promising tool to suppress gene expression in mammalian cells. In this regard, this project involves the transfection of human bone marrow MSCs and MCF-7, a human breast adenocarcinoma cell line, with small-interfering RNA (siRNA), synthesized in house or expressed as a short-hairpin RNAs (shRNAs) from minicircle (MC) vectors, that target VEGF expression. Overall, RT-qPCR results revealed a VEGF-mRNA knockdown of 50% and 40% after synthetic siRNA transfection of MSCs and MCF-7, respectively. Similarly, ELISA results indicate a decrease in VEGF secretion. Regarding transfection results with MC vectors, similar results were expected, however, increased VEGF expression was consistently found at mRNA and protein levels after MSCs and MCF-7 cells transfection. Although further studies are required, these discrepancies appear to be related to the incorrect processing of the transcribed shRNA into a functional siRNA. Overall, this study provides insights regarding the implementation of an siRNA-based system that targets VEGF expression, aiming at slowing down tumour angiogenesis.

Keywords: *Tumour angiogenesis; Mesenchymal Stem/Stromal Cells; Vascular Endothelial Growth Factor; RNA interference*

INTRODUCTION

Angiogenesis is the growth or formation of new blood vessels from pre-existing vasculature. It involves a complex and dynamic interaction between endothelial cells (ECs) and the corresponding extracellular environment in which the balance between angiogenic activators and angiogenic inhibitors tightly controls the rate of blood vessel formation.^{1,2} This process begins *in utero* and prolongs throughout life, occurring both in health and disease. It has a major role in reproduction, as it occurs naturally in the placenta and uterus during pregnancy and in the ovary during follicle development, ovulation and corpus luteum formation.² Another instance in which it occurs later in life is in regeneration of damaged tissues during the wound healing in healthy adults.^{2,3} Nevertheless, several diseases include excessive or deficient angiogenesis as part of the pathology, as the balance between stimulant and inhibitory angiogenic factors is often disturbed. In conditions such as cancer and other non-malignant conditions, like macular degeneration, the prevention of new forming blood vessels is highly desirable as a therapeutic strategy.^{2,3} In fact, tumour angiogenesis is one of the hallmarks in cancer progression.^{4,5} In growing cancers, tumour-infiltrating cells of haematopoietic and non-haematopoietic origin, such as bone marrow (BM)-derived endothelial or

mesenchymal progenitors are recruited from the BM to the tumour via the systemic circulation. Additionally, tissue-resident cells are also recruited, including ECs, pericytes, fibroblasts and adipocytes.⁴ Together, the broad range of signals secreted by tumour-associated cells, such as IL-1 β , IL-6, FGF-2, TNF- α and vascular endothelial growth factor (VEGF), and the extracellular matrix in which they are embedded sustain angiogenesis throughout the subsequent phases of tumour progression.⁴ Additionally, vessel growth is not only stimulated but can lead to the formation of abnormal vessels in terms of structure and function, including unusual leakiness, potential for rapid growth and remodelling, high tortuosity and sinusoidal appearance, poor coverage by vascular supportive cells and incorporation of tumour cells into the endothelial wall.⁵ Abnormal tumour vessels can also contribute to the resistance of tumour cells to common therapies since they obstruct the function of immune cells in tumours, as well as the transport and distribution of chemotherapeutics.^{2,6} Besides that, these phenotypes mediate the dissemination of tumour cells in the bloodstream and sustain the pathological characteristics of the tumour microenvironment.⁵ Mesenchymal Stem/Stromal Cells (MSC) are a diverse subset of adult, fibroblast-like, multipotent precursors capable of differentiate into tissues

of mesodermal origin. MSCs are present in perivascular locations providing stromal support to the maintenance of a dynamic and homeostatic tissue microenvironment, mainly by the secretion of biologically active molecules that exert beneficial effects on other cells, namely minimizing apoptosis, inducing angiogenesis, support of proliferation and differentiation of progenitors/stem cells and recruitment of endogenous cells.⁷⁻¹⁰ These cells exhibit a tropism to injured tissues and also several types of tumours, and upon with the tumour microenvironment, MSCs became active participants in tumour development, namely by promoting angiogenesis.^{11,12} VEGF, is one of the most important factor in angiogenesis, being responsible for the stimulation of EC's functions needed for new blood vessel formation, generally by inducing EC proliferation, survival, migration, and differentiation.¹³ This factor also potentiates vascular permeability, which can both precede and accompany angiogenesis.^{13,14} VEGF is present in tumour microenvironment being secreted by cancer and surrounding cells, such as MSCs. Thus, blocking VEGF production seems a plausible approach to slow down tumour growth. Overall, a promising tool for blocking VEGF production by MSCs and cancer cells is by the use of RNA interference (RNAi) technology, a post-transcriptional gene-silencing pathway that involves the double-stranded RNA (dsRNA)-mediated degradation of target mRNA. The effectors molecules of the pathway are 21- to 23-nucleotide short interfering RNAs (siRNAs). siRNA staggered duplexes with 2-nucleotide overhangs at the 3'-terminii are produced following ATP-dependent processive cleavage of long dsRNAs by the enzyme Dicer. The antisense strand of the siRNA is then incorporated into an RNA-induced silencing complex (RISC) and used to target perfectly complementary mRNA species. RISC cleaves the target mRNA, 10 nucleotides from the 5' end of the incorporated siRNA strand.¹⁵ An alternative method for gene silencing in mammalian cells through a RNAi-related process has also been developed, involving the use of expression vectors that produce short-hairpin RNAs (shRNAs), that can silence gene expression as effectively as do synthetic siRNAs.^{15,16} Despite the challenges with silence efficiency, delivery and possible harmful off-target effects,^{17,18} synthetic siRNAs have been widely used for loss-of function phenotype analyses in mammalian cells and extensively studied as their therapeutic potential by blocking the synthesis of disease-causing proteins. In this context, this project involves the transfection of human bone marrow MSCs and MCF-7, a human breast adenocarcinoma cell line, with specific siRNAs targeting VEGF expression. siRNAs will be designed and synthesized outsourced with specific chemical modifications to increase their half-lives. Additionally, minicircle (MC) vectors encoding a short hairpin RNA

(shRNA), targeting the same location of VEGF-mRNA, will be also constructed, produced and purified for further transfection. Unlike the synthetic siRNA, which is degraded with gene silencing, the MC continues to deliver the transcribed shRNA to the transfected cells. Moreover, to assess VEGF silencing, VEGF-mRNA and VEGF-protein will be quantified by real time quantitative PCR and ELISA, respectively. Finally, the effect on blood vessel formation will be addressed by performing a functional in vitro assay, in which the capacity of human umbilical vein endothelial cells (HUVECs) to form tubes in the presence of the conditioned media of transfected MSCs and MCF-7 will be evaluated.

MATERIALS AND METHODS

In silico design of a siRNA and vector-expressed shRNA that silences VEGF expression

The oligonucleotide sequence of siRNA targeting VEGF chosen was: Passenger/Sense: AUGUGAAUGCAGACCAAAGdTdT; Guide/Antisense: CUUUGGUCUGCAUUCACAUUU which is shown to efficiently silence VEGF expression in different mammalian cells.¹⁹⁻²¹ The inclusion of the deoxythymidine dinucleotide overhangs in the passenger strand should improve strand selection, since RISC exhibit a distinct preference in favour of a strand with an RNA overhang (guide strand).²² Additionally, siRNA will be expressed as a shRNA encoded in a minicircle DNA vector. The inserted fragment must contain the sequence of the passenger strand followed by a loop sequence and finally the sequence of the guide strand, allowing the transcript to fold back on itself forming a shRNA, analogous to natural miRNA.²³ For the loop sequence the 9-nt loop 5'-TTCAAGAGA -3' was selected since is one of the most commonly used hairpin loops and is based on a naturally occurring miRNA sequence.²⁴ A graphical representation of the annealed insert, the transcript and its hairpin structure can be observed in Figure 1.

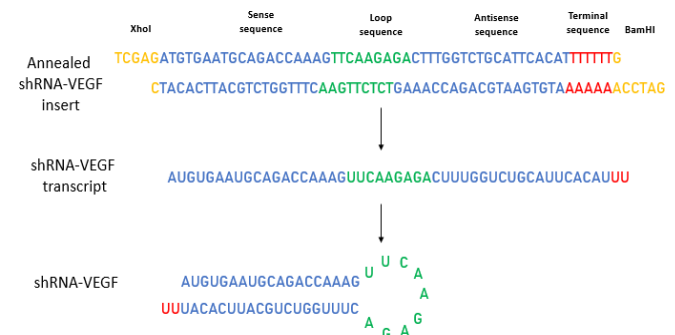


Figure 1- Graphical representation of the annealed insert, the transcript and its hairpin structure originating the shRNA.

Construction of parental plasmids expressing a shRNA targeting VEGF

pshRNA

A pair of DNA oligonucleotides (STABVIDA) (Forward: TCGAGATGTGAATGCAGACCAAAGTTCAAGAGACTTTGGTCTGCATTCACATTTTTTTTG; Reverse: GATCCAAAAAATGTG AATGCAGACCAAAGTCTCTTGAACCTTTGGTCTGCATTCACA TC) were resuspended in 10 mM Tris, pH 8.0; 50 mM NaCl; 1 mM EDTA²⁵, each obtaining a final concentration of 10µM. The annealing was performed by incubation of 20µL of each oligonucleotide at 95°C for 2 min, then it was gradually cooled to 25 °C during 45 min, and finally cooled to 4°C for temporary storage.²⁵ After the annealing, the dsDNA oligonucleotide exhibit overhangs of the XhoI and BamHI digested sequence, as shown

in Figure 1. The parental plasmid pVEGF-GFP, previously developed at iBB-BERG laboratory²⁶, was digested with XhoI (*Thermo Fisher Scientific*) and BamHI (*Promega*) restriction enzymes. Then, the digested pDNA was separated by a 1% agarose gel electrophoresis and the correct fragment was extracted from the gel with NZYGelpure kits (*Nzytech*). Afterwards, the annealed dsDNA oligonucleotide (insert) was ligated to the XhoI/BamHI digested vector pVEGF-GFP using T4 DNA Ligase (3U/ μ L; *Promega*). After *E. coli* DH5 α transformation by heat shock, cells were plated in a LB agar medium supplemented with 30 μ g/mL kanamycin (*Sigma-Aldrich*) which is the selection marker of the plasmid, and incubated overnight at 37°C. *E. coli* DH5 α transformants were grown overnight in 15 mL Falcon tubes containing 5 mL of LB medium supplemented with 30 μ g/mL kanamycin (*Sigma-Aldrich*). The pDNA was extracted by NZYMiniprep kit (*Nzytech*) and digested with the restriction enzymes SpeI (*Fermentas*) and BamHI (*Promega*) to verify the insertion. To further validation, DNA sequencing was performed on the construct (STABVIDA), confirming the sequence of the insert. Finally, 25 ng of purified pshRNA was used to transform 100 μ L chemically competent *E. coli* BW2P by heat shock. Aliquots of 35 μ L of 35% (w/v) glycerol and 65 μ L of culture were made and kept at -80°C.

pshRNA 2

In addition to pshRNA, a parental plasmid with a different sequence for the CMV promoter and a synthetic polyA signal instead of the BGH polyadenylation signal, was also constructed. Firstly, PCR amplification of the insert was performed using the KOD Hot Start DNA Polymerase kit (*Novagen*), using the DNA oligonucleotides as primers/template (STAVIDA) (Forward: CCAGAGCTCGGTTTGTAGTGAACCGTCTCGAGATGTGAATGCAGACCAAAGTTCAAGAGACTTTGGTCTGCATTACATTTTTTACTAGTAATAAAGGAT; Reverse: CTGATGCATCCGCGGGGACTAGAGTGCACGCGGCCGCACACAAAAACCAACACACGGATCCAATGAAAATAAAGGATCC TTTATTACTAGTAAAA). The cycling conditions were an initial denaturation at 95°C for 2 min, followed by 35 cycles of 1 min at 95°C, a cooling ramp of 1.10 min from 60°C to 44°C and 1 min at 70°C. After amplification, the PCR product was separated by a 1% agarose gel electrophoresis and the fragment was extracted with NZYGelpure kits (*Nzytech*). Afterwards, the PCR product was digested with SacI (*Thermo Fisher Scientific*) and NsiI (*Promega*) and following purified with NZYGelpure kits (*Nzytech*). Parallely, the previously constructed parental plasmid pshRNA was digested with SacI (*Thermo Fisher Scientific*) and NsiI (*Promega*). The digested pDNA was separated by a 1% agarose gel electrophoresis and the correct fragment was extracted with NZYGelpure kits (*Nzytech*). The ligation mixture was performed using T4 DNA Ligase (3U/ μ L; *Promega*). After *E. coli* DH5 α transformation by heat shock, cells were plated in a LB agar medium supplemented with 30 μ g/mL kanamycin (*Sigma-Aldrich*). The screening of candidates was performed as previously, using the restriction with SacI (*Thermofisher*) and DNA sequencing to validate the insertion. Finally, 25 ng of purified pshRNA_2 was used to transform *E. coli* BW2P and aliquots of the transformants were performed as described before.

Parental plasmid and minicircle production

The producer strain *E. coli* BW2P was constructed by the insertion of the PBAD/*araC-parA* cassette in the *endA* gene in the genome of the *E. coli* strain BW27783 (The Coli Genetic Stock Center at Yale). The cassette contains the ParA resolvase gene under a PBAD promoter with an optimized ribosome binding site and the AraC repressor gene in opposite direction.²⁷ ParA catalyzes the recombination of parental plasmid (PP) into miniplasmid (MP) and minicircle (MC)²⁸ in which the activity is induced by arabinose and repressed by glucose. Thus, this strain was used to produce the MC vectors. After overnight incubation at 37 °C and 250 rpm, cells were used to inoculate 100 mL

Erlenmeyer flasks containing 30 mL of the previously described medium at an OD_{600nm} \approx 0.1. Cultures were incubated at 37 °C and 250 rpm until OD_{600nm} \approx 2.5 has been reached. At that point, an appropriate volume was used to inoculate 2 L Erlenmeyer flasks containing 250 mL of the previously described medium at an OD_{600nm} \approx 0.1. The OD_{600nm} was monitored during the growth and recombination induction was performed at an OD_{600nm} of approximately 2.5 (late exponential phase). The recombination was induced by adding 0.01% (w/v) L-(+)-arabinose directly to the culture and recombination was allowed to proceed for 1 and 2 hours. Culture samples at the induction time and during induction were collected to monitor recombination profile by agarose gel electrophoresis. The final culture was centrifuged for 15 minutes at 4°C under 6000xg. The cell pellets were stored at -20°C for further purification.

Purification of minicircles

Primary purification

The process was based in the method described by Silva-Santos *et al* (2017)²⁹. Firstly, an alkaline lysis was performed to the cell pellets stored at -20°C. Briefly, the pellets were resuspended in P1 buffer (50 mM glucose, 25 mM Tris-HCl, 10 mM EDTA, pH 8) by vortex. The volume of P1 (V_{P1}): was calculated to have a cell suspension with an OD_{600nm} = 60. The following equation was used, considering the final optical density of the culture (OD_{600nm}) and volume of the respective cellular growth (V_{cg}):

$$V_{P1} = \frac{OD_{600nm} \times V_{cg}}{60}$$

(Equation 1)

The resuspended cells were mixed gently with P2 buffer (0.2 M NaOH, 1% (w/v) SDS) at a 1:1 volume ratio and incubated at room temperature for 10 minutes. Finally, the P3 buffer (5 M acetate; 3 M potassium, pH 5) at a 1:2 volume ratio was added. The mixture was gently homogenized and placed on ice for 10 minutes. After neutralization, the mixture was centrifuged twice at 18250xg and 4°C for 30 minutes. The nucleic acids of the clarified lysate obtained were precipitated with 0.7% (v/v) isopropanol at -20°C for 2 hours. Afterwards, a centrifugation at 18250xg and 4°C for 30 minutes was performed. The resulting pellets were left to dry overnight at room temperature. The pellets were resuspended in 10mM Tris-HCl, and then conditioned with ammonium acetate salt for a final concentration of 2.5M. After salt dissolution, the lysate was placed on ice for 15 minutes and centrifuged at 15000xg and 4°C for 30minutes. The supernatant was recovered and 30% (w/v) PEG-8000 in 1.6 M NaCl at a 1:2 volume ratio was added and left overnight at 4°C. Afterwards, the mixture was centrifuged at 15000xg, 4°C for 30 min, and the pellet containing the nucleic acids was washed with 70% ethanol and centrifuged again. The pellet was left to dry and finally resuspended in PCR-grade water.

Digestion with endonuclease Nb.BbvCI

The digestion step was carried out as described in Alves *et al* (2016)³⁰ with endonuclease Nb.BbvCI to nick of one of the strands of the MP and of the non-recombined PP, since this enzyme recognizes a specific target sequence strategically placed in the MP molecule. The sample obtained previously was divided in two and the digestion was performed in a total reaction volume of 290 μ L, using 5-10 μ L of Nb.BbvCI (1U/ μ L, New England Biolabs), 1x CutSmart buffer (New England Biolabs), for 1 to 3 hours at 37°C. The digested samples were analyzed by agarose gel electrophoresis.

Multimodal chromatography

The Multimodal chromatography based in the method described by Silva-Santos *et al* (2017)²⁹ was performed using a Tricorn 10/50 column (GE Healthcare) packed with 5 mL of Capto™ adhere resin connected to an ÄKTApurifier10 system (GE Healthcare) under the control of UNICORN 5.11 software. This matrix contains an immobilized ligand that can mediate anion-exchange (with the charged nitrogen), hydrophobic (with the phenyl ring) and hydrogen bonding (with the hydroxyl groups)

interactions with the solutes in the feed stream. The samples were conditioned with a buffer containing 830 mM NaCl in 10 mM TE, prior to column loading. The mobile phase consisted of mixtures of buffer A (10 mM Tris-HCl, 1 mM EDTA, pH 8) and buffer B (2 M NaCl in 10 mM Tris-HCl, 1 mM EDTA, pH 8). The absorbance of the eluate was continuously measured at 254 nm by a UV detector positioned after the column outlet and the system was operated at 1 mL/min. The column was equilibrated with 3 column volumes (CV) of 41.5% buffer B (approximately 69 mS/cm). Then, 1 mL of the conditioned sample was injected into the column by washing the loop with 3 mL of 41.5% buffer B. All unbound material was washed out of the column with 2 CV of 41.5% buffer B. Elution steps were then performed with 3 CV of 46% B (approximately 75 mS/cm) and 3 CV of 100% B (approximately 140 mS/cm). The eluate was collected (fractions of 1.5 mL) during the chromatographic run in 2 mL Eppendorf tubes with a fraction collector. The fractions collected were analyzed by agarose gel electrophoresis.

Dialysis and Concentration

Finally, MC purified fractions were processed in Amicon® Ultra-4, MWCO 30 kDa (Thermo Fisher Scientific), according to the respective protocol, to dialyze and concentrate the sample. Afterwards, the purified pDNA remained approximately in 100 µL of PCR-grade water and was stored at 4°C. The concentration pDNA was assayed by spectrophotometry at 260nm, using Nanodrop Spectrophotometer (GE Healthcare), and pDNA integrity and purity was assessed using agarose gel electrophoresis.

Bone Marrow Mesenchymal Stem/Stromal Cells thawing and expansion

BM-MSCs (M79A15 and M48A08 donors) kept cryopreserved in liquid/vapor phase nitrogen tanks at the iBB-SCERG, were thawed by submerging the cryovials in a 37°C water bath and resuspended in Dulbecco's Modified Eagle's Medium (DMEM) supplemented with 20% fetal bovine serum (FBS) (Thermo Fisher Scientific). After a centrifugation at 1500xg for 7 min, the pellet was resuspended in DMEM supplemented with 10 % FBS MSC qualified (Thermo Fisher Scientific) and 1 % Antibiotic-Antimycotic (A/A, Gibco). The determination of total cell number (TCN, Equation 2) and viabilities (CV, Equation 3) was estimated by the 0.4% Trypan Blue dye exclusion method using a hemocytometer under an optical microscope.

$$TCN = \frac{\text{Number of viable cells}}{\text{Number of squares}} \times 1000 \text{ cells/mL} \times \text{Dilution factor} \times \text{Final volume}$$

(Equation 2)

$$CV(\%) = \frac{\text{Number of viable cells}}{\text{Total number of cells}} \times 100$$

(Equation 3)

According to the cell number, the cells were plated in T-Flasks at the appropriate cell density (3,000 – 6,000 cells/cm²) in the previously described culture medium. Cells were incubated at 37°C, 5% CO₂ and >95% humidity and the culture medium was replaced every 3-4 days. Cell passages were performed when 70-80% confluence was observed by microscope. Briefly, the exhausted medium was removed, and cells were washed with Phosphate Buffered Saline (PBS) buffer. After PBS removal, cell detachment was accomplished by adding accutase (Thermo Fisher Scientific) solution, for 7 min at 37°C. Inactivation of the accutase enzymatic activity was achieved by adding DMEM supplemented with 10% FBS in a proportion of 1:1. Collected cells were concentrated by centrifugation at 1500xg for 7 min and resuspended in fresh medium. Cell number and viability were accessed by the Trypan Blue dye exclusion method and the appropriate cell densities were plated.

MCF-7 thawing and expansion

Cryopreserved MCF-7 (human breast adenocarcinoma cell line) cells were thawed using the same procedure as BM-MSCs thawing above described. Vials containing 1 x 10⁶ cells were plated in T-Flask with 25 cm² in high glucose DMEM

supplemented with 10 % FBS (Thermo Fisher Scientific) and 1 % A/A (Gibco). Cells were incubated at 37°C, 5% CO₂ and >95% humidity. Typically, part of the cells remained detached and were removed by replacing medium in the following day. Cell passages were performed when 90-100% confluence was observed by microscope. Firstly, the exhausted medium was removed, the cells were washed with PBS buffer and detached by adding 0.05% trypsin (Coring) for 3 min at 37°C. Inactivation of the trypsin enzymatic activity was achieved by adding DMEM supplemented with 10% FBS in a proportion of 2:1. Collected cells were concentrated by centrifugation at 1500xg for 7 min and resuspended in 3 mL fresh medium. Finally, 1 mL of the medium was plated in T-Flask with the same area. Cell number and viability were accessed by the Trypan Blue dye exclusion method and the appropriate cell densities were plated when used in transfection experiments (25,000 cells/cm²).

Liposome-mediated transfection of BM-MSCs and MCF-7

The process was based in the method described by Boura *et al* (2013)³¹. BM-MSCs from P4-P7 were plated at a cell density of 4,000 cells/cm² in 12-well plates and cultured in the appropriate culture medium. Alternatively, for MCF-7 transfection, cells were plated at a cell density of 25,000 cells/cm². After 72 hours of culture, with cells at 70-80% confluence, transfection was carried out using the 1 mg/mL Lipofectamine 2000 reagent (Invitrogen) according to the manufacturer's instructions. Briefly, the appropriate amount of MC (MC-VEGF-GFP; MC-shRNA; MC-shRNA_2) or synthetic siRNA and 1 µL of lipofectamine were diluted in 50 µL of Opti-MEM® medium (Thermo Fisher Scientific). Then, solutions were combined to allow complex formation to occur during 20 minutes at room temperature. After the 20 minutes incubation, the transfection mixture was added to the cells in which the medium was replaced to 400 µL of serum- and antibiotics free DMEM. Five hours after transfection the medium was replaced with 1 mL of fresh medium. Cell pellets and culture supernatants were collected to further experiments at different time points, namely 24, 48 and 72 hours after transfection. Before -80°C storage, culture supernatants were centrifuged at 2000xg for 10 min and cells were centrifuged at 1500xg for 7min. Both non-transfected cells and cells treated only with lipofectamine were used as a control. Besides the previous described calculations of the cell number and cell viability, for each transfection sample (*t*), cell recovery (*CR*) was calculated by Equation 4, where *CA* is the number of viable cells and *c* is the non-transfected control cells. After centrifugation at 1500xg for 7min, the cells pellets were kept at -80°C to further experiments.

$$CR_t(\%) = \frac{CA_t}{CA_c} \times 100$$

(Equation 4)

RNA extraction, conversion to cDNA and VEGF-mRNA quantification by RT-qPCR

Total RNA was extracted from the cell pellets with RNeasy Mini Kit (Qiagen). Afterwards, 250-500 ng of RNA were converted to cDNA with iScript™ cDNA Synthesis Kit (BIORAD), using an equal RNA mass for all the samples within an experiment. The PCR conditions included a single cycle of 5 minutes at 25°C, 30 minutes at 42°C and 5 minutes at 85°C. As an alternative, the High Capacity cDNA Reverse Transcription Kit (Thermo Fisher Scientific) was used, in which the PCR conditions were a single cycle of 10 minutes at 25°C, 120 minutes at 37°C and 5 minutes at 85°C. cDNA samples were stored at -20°C. Real-time quantitative PCR (RT-qPCR) was performed using Applied Biosystems StepOne Real-Time PCR System (Applied Biosystems), using NZY qPCR Green ROX plus kit (Nzytech) with a reaction mixture composed by either 0.4 µM of primers for VEGF (Forward: CGAGGGCCTGGAGTGTGT, Reverse: CGCATAATCTGCATGGTGATG) or for the control GAPDH (Forward: ACGACCCCTTCATTGACCTCA, Reverse: ATATTTCTCGTGGTTCACACC), 25 ng of cDNA template and 1x NZY qPCR Green Master Mix to a final volume of 20 µL. Each

PCR run was followed by a no-template control to confirm the specificity of the amplification and the absence of primer dimers. The relative gene expression from quantification cycle (Ct) values obtained by RT-qPCR was calculated by the $\Delta\Delta Ct$ method. Overall, this is accomplished by normalization of a target gene (VEGF) with experimental treatment, to an endogenous control gene (Glyceraldehyde 3-phosphate dehydrogenase; GAPDH) whose expression remains unchanged. Subsequently, this value is normalized to the targeted gene expression detected in a separate control sample. The fold change (FC) and percentage of knockdown (%KD) of the target gene in the treated cells, the following equations were used:

$$FC = 2^{-\Delta\Delta Ct}; \%KD = (1 - 2^{-\Delta\Delta Ct}) \times 100$$

(Equation 7 and 8)

VEGF quantification by ELISA

BM-MSC and MCF-7 culture supernatants collected 48h post-transfection were centrifuged as previously described and stored at -80°C to further VEGF quantification by Enzyme-Linked Immunosorbent Assay (ELISA). VEGF quantification was performed using RayBio® Human VEGF ELISA kit (RayBiotech), accordingly to manufacturer's instructions. Afterwards, the standard curve was generated, and the concentration of each sample was determined based on that calibration curve. VEGF secretion (VGF pg/1000 cells) in each sample was assessed considering its initial volume, and cell number of the correspondent culture supernatant. The values were expressed as the mean of duplicates of one single experiment.

In vitro tube formation assay

As an attempt to evaluate the MSC angiogenic potential after transfection, a functional assay with HUVEC was performed – *in vitro* tube formation assay. For that, 24h after transfection, the medium was replaced by Endothelial Growth Basal Medium - 2 (EBM-2, Lonza) and cells were allowed to condition the medium for 48 hours. The CM was then collected, centrifugated for 10 min at 2000xg and stored at -80°C until used in the tube formation assays. CM were produced from at least 1.0×10^5 cells and it was normalized to cell number 72 h after transfection. Firstly, in a 96-well plate the wells were coated with 50 μ L of Matrigel (100mg/mL, Corning) per well and incubated for 30min at 37°C. After centrifugation at 1500xg for 7 min, 20,000 HUVECs were resuspended in 200 μ L of MSCs CM, EBM-2 as negative control, or Endothelial Cell Growth Medium-2 (EGM-2, Lonza) as positive control. Finally, cells were plated in the wells and after 6 hours of incubation at 37°C the HUVECs tube formation was evaluated (tube connections and number of tubes), using the ImageJ software.

RESULTS AND DISCUSSION

Construction of parental plasmid expressing a shRNA targeting VEGF (pshRNA)

Despite the majority of studies that developed a short-hairpin RNA expressing system used viral vectors, mainly due to their high delivery efficiencies and stable gene expression, safety concerns are still a limitation³², and in the present work, a non-viral system was selected. Minicircle DNA vectors, free of plasmid bacterial DNA sequences, capable of persistent high level of transgene expression *in vivo*, seemed to be a promising choice.^{28,33} For that, a parental plasmid containing the bacterial backbone to allow bacterial replication, and the eukaryotic expression cassette (shRNA sequence) flanked with MRS to the further minicircle isolation, was constructed – pshRNA. Therefore, to construct the parental plasmid expressing a shRNA targeting VEGF, pVEGF-GFP, a PP

developed previously at iBB-BERG laboratory²⁶, was used as a template in which the fusion between VEGF and GFP genes was replaced by the annealed dsDNA oligonucleotides (Figure 1). The selected targeting sequence of shRNA was chosen based on its efficiency in silence VEGF expression in different mammalian cells.^{19–21} After pVEGF-GFP double digestion with XhoI and BamHI and ligation of the desired fragment of pVEGF-GFP with the annealed dsDNA oligonucleotides, *E. coli* DH5 α cells were transformed. Six colonies that resulted from the transformation were selected from the plate to further evaluation. After pDNA extraction and digestion with SpeI and BamHI restriction enzymes, the pDNA was separated on an agarose gel electrophoresis (Figure 2).

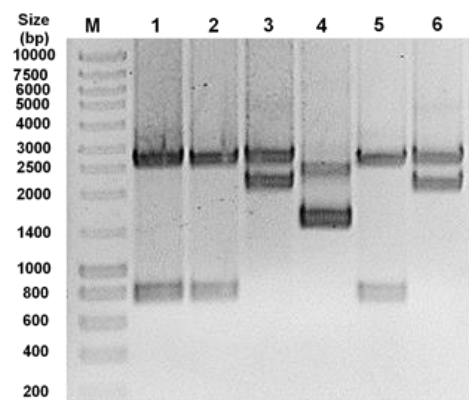


Figure 2 - Agarose gel electrophoresis analysis of pshRNA candidates. pDNA purified from *E. coli* colonies resulting from the transformation with the ligation mixture. The samples were digested with SpeI and BamHI for 3h at 37°C. Lane M - molecular weight marker NZYDNA Ladder III (Nzytech)

The restriction pattern of the transformants 1, 2 and 5 matches the one expected for the digestion of the newly constructed PP (pshRNA) with SpeI and BamHI (2,553 bp + 751 bp) while transformants 3 and 6 matches the restriction pattern of double digested pVEGF-GFP (2,553 bp + 2,010 bp). The transformant 1 inserted sequence was confirmed by DNA sequencing (*data not shown*), in which the result validated the correct insertion of the shRNA sequence and consequently successful construction of the parental plasmid pshRNA.

pshRNA minicircles production and purification

For the production and *in vivo* recombination of the parental plasmid, the producer strain *E. coli* BW2P was used. This strain contains the ParA resolvase gene under transcriptional control of the arabinose promoter/operator system, induced by arabinose and repressed by glucose. ParA catalyzes to recombination of parental plasmid (PP) into miniplasmid (MP) and minicircle (MC).²⁸ *E. coli* BW2P cells harbouring pshRNA were grown and OD_{600nm} was monitored throughout time allowing the construction of growth curves (*data not shown*). The recombination into MC plus MP was induced by the addition of L-(+)-arabinose at an OD_{600nm} \approx 2.5, corresponding to the late exponential phase to allow cell number and PP maximization before induction. To evaluate the

recombination efficiency of newly constructed PP pshRNA, samples were collected after recombination induction, every 30 minutes for 2 hours. The pDNA was extracted from the samples and separated by an agarose gel electrophoresis (Figure 3). This analysis showed that before induction, open-circular (sc) PP bands predominate

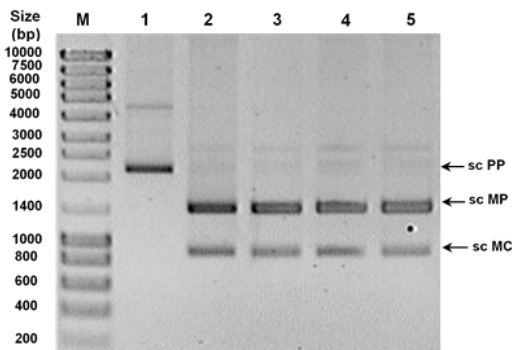


Figure 3 - Agarose gel electrophoresis analysis of pshRNA recombination *in vivo*. pDNA purified from *E. coli* cells collected before (lane 1) and after (lane 2: 30min, lane 3: 60min, lane 4: 90min, lane 5: 120min) induction of recombination with L-(+)-arabinose. Lane M - molecular weight marker NZYDNA Ladder III (Nzytech). Abbreviations: sc PP- supercoiled parental plasmid; sc MC- supercoiled minicircle; sc MP- supercoiled miniplasmid.

(lane 1, Figure 3). The fact that MC and MP species are absent is a clear indication that no recombination occurs before L-(+)-arabinose induction. On the other hand, after 30min, 60min 90min, and 120min of recombination, the production of MP and MC is detected by the presence of the corresponding bands of sc MP at ~1,500bp and of sc MC at ~900bp and absence of the PP bands (lane 2 to 5, Figure 3). From this result, it is possible to confirm the high recombination efficiency of the producer system used to express the ParA resolvase, since PP species are almost undetectable after 30min of recombination (lane 2, Figure 3). After *E. coli* BW2P growth and recombination of PP into target MC, cell harvesting followed by alkaline lysis were performed, to release the intracellular contents and denature genomic DNA and proteins. Then, a tandem precipitation process was performed with isopropanol, ammonium acetate and PEG-8000, in order to remove the RNA and protein impurities of the solution and concentrated the pDNA. Samples were collected after each precipitation step to monitor the primary purification of pshRNA minicircle (MC-shRNA) (Figure 4). Afterwards, enzymatic digestion with Nb.BbvCI, that recognizes a specific target sequence located on the bacterial backbone of the PP, was used to convert sc molecules into the corresponding oc forms by nicking one of the MP and non-recombined PP strands at the target site.³⁰ Samples collected before and after digestion with Nb.BbvCI for 1 hour at 37°C, were analysed through agarose gel electrophoresis (Figure 4). Through the gel electrophoresis analysis, it was possible to verify that the two isoforms of MPs and MCs and RNA are the major components in the samples (Figure 4). Additionally, the RNA load was substantially reduced after ammonium

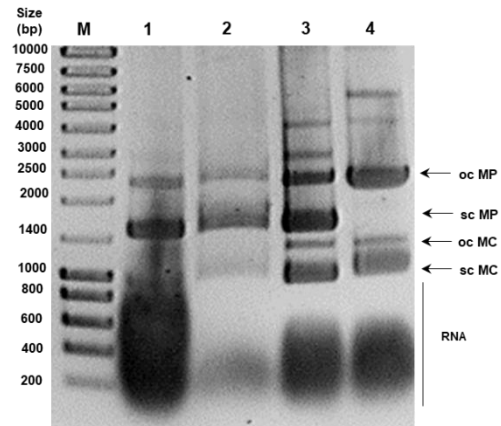


Figure 4 - Agarose gel electrophoresis was used to analyse each step of the primary purification of pshRNA₂ minicircle and subsequent digestion with endonuclease Nb.BbvCI. Samples were collected after each step of the primary purification: alkaline isopropanol precipitation (lane 1, 3µL of sample), ammonium acetate precipitation (lane 2, 6µL of sample), PEG-8000 precipitation (lane 3, 0.5 µL of sample) and after (lane 2, 1µL of sample) digestion with endonuclease Nb.BbvCI.. Lane M - molecular weight marker NZYDNA Ladder III (Nzytech). Abbreviations: oc MC- open-circular minicircle; sc MC- supercoiled minicircle; oc MP- open-circular miniplasmid; sc MP- supercoiled miniplasmid.

acetate precipitation (lane 3, Figure 4). However, it is possible to note that high amounts of RNA molecules from various sizes appear to remain in the sample (lane 3, Figure 4), that could lead to complications in the following purification steps. The high amount of RNA might be due to an inadequate RNA degradation during cellular lysis or some precipitation step poorly executed, namely during the precipitation with ammonium acetate where RNA and protein impurities in this solution should be excluded in the pellet.²⁹ Regarding the Nb.BbvCI, digestion, the results show that sc MP (lane 3, Figure 4) were readily converted into its oc counterpart (lanes 4, Figure 4), whereas sc MC remained intact (lanes 3 and 4, Figure 4). After digestion, the sample comprised a mixture of sc MC, oc MC and oc MP (lanes 4, Figure 4).

In order to isolate the sc MC from the other species, multimodal chromatography was completed using a 5 mL chromatographic column packed with Capto™adhere resin. Runs were performed at 1 mL/min, unbound material was washed with 2 CV of 41.5% B (830 mM, ≈ 69 mS/cm) and elution was accomplished using two steps with increasing salt concentration, the first at 46% B (920 mM, ≈75 mS/cm) and the second at 100% B (2 M, ≈140 mS/cm). The chromatogram obtained is shown in Figure 5A. Moreover, some of the fractions collected were analysed by agarose gel electrophoresis (Figure 5B). the results show that the first peak, at 41.5%B, contains oc forms of MP and MC (lanes 2–5), the second peak, at 46%B contains sc MC (lanes 13–17) and a last peak at 100%B contains RNA (lane 25). The fraction 13 to 15, appear to be free from oc species and RNA, containing only sc MC. The chromatographic profile obtained (Figure 5A) is similar to the one expected²⁹, however is possible to note that the second peak is inferior and the sc MC bands are fainter (Figure 5B), indicating low amounts of pDNA. Afterwards, dialysis and concentration of the

fractions 13-15 of the chromatographic runs was accomplished using Amicon® Ultra-4 MWCO 30 kDa,

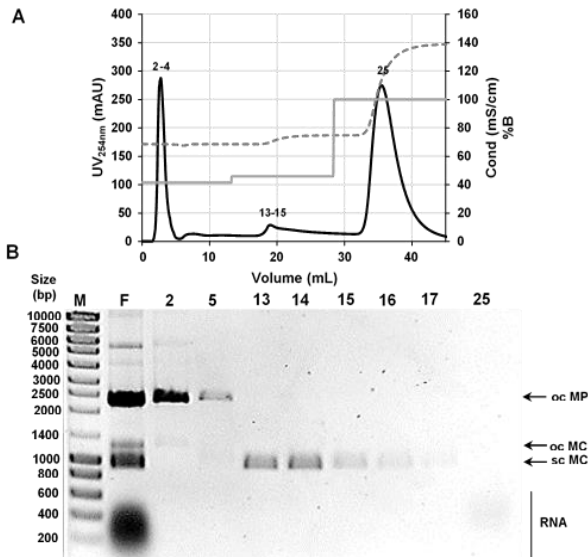


Figure 5- Multimodal chromatography purification of sc MC from pshRNA from a feed stream containing also oc pDNA and RNA. **(A)** Chromatogram obtained using a Capto™ Adhere column and a series of elution steps with increasing NaCl concentrations. Numbers over peaks correspond to collected fractions. Black continuous line: absorbance at 254 nm; grey dashed line: conductivity (mS/cm); grey continuous line: percentage of buffer B (%B). **(B)** Agarose gel electrophoresis analysis of fractions collected during the chromatographic run. The numbers above each lane correspond to fractions collected (10 µL of sample for fractions 2–17; 30 µL of sample for fraction 25). Lane M - molecular weight marker NZYDNA Ladder III (Nzytech). Abbreviations: oc MC- open circular minicircle; sc MC- supercoiled minicircle; oc MP- open circular miniplasmid; sc MP- supercoiled miniplasmid.

Lipofection of BM-MSCs with the MC-shRNA and synthetic siRNA

In order to evaluate the silencing potential of the siRNA and MC-derived shRNA, a transfection experiment of BM-MSCs using the Lipofectamine reagent was performed. BM-MSCs were lipofected according to Materials and Methods, with 1 µg MC-shRNA/ 50nM synthetic siRNA. Non-transfected cells and cells transfected without pDNA/siRNA were used as control. Cells were collected 24h and 48h post-transfection. Afterwards, the collected cells were used to quantify the VEGF-mRNA, by RT-qPCR using the $2^{-\Delta\Delta Ct}$ method (Figure 6).

Though the analysis of Figure 6, it is possible to note that the transfection of the MC-shRNA exhibited 6.7- and 15-fold higher mRNA copies of VEGF than the control cells (MSC LF), 24h and 48h after transfection respectively. The results are contrary to the expected, since the transcribed shRNA should be processed into a siRNA that recognizes a specific region of the VEGF-mRNA targeting it for degradation, leading to reduced levels of VEGF, instead of inducing its expression as observed in these preliminary experiments. Alternatively, it is possible to verify that the transfection with the synthetic siRNA induce an effect in silencing VEGF-mRNA expression with a knockdown of approximately 38%. With the observation that the synthetic siRNA successfully leads to the silencing of VEGF-mRNA, it is possible to conclude that the selected

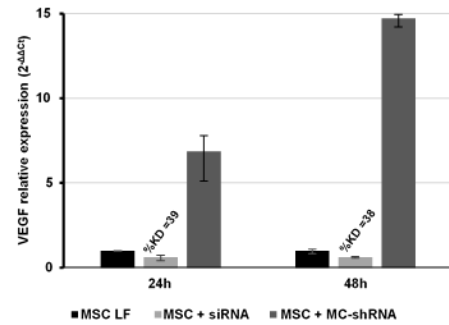


Figure 6- Evaluation of transgene delivery 24 and 48 hours after lipofection with MC-shRNA or synthetic siRNA, by analysis of BM-MSC VEGF gene expression by RT-qPCR. The values were obtained using $2^{-\Delta\Delta Ct}$ method, with GAPDH as the endogenous control gene and MSC transfected without pDNA/siRNA, collected after 24h and 48h, as baseline. The percentages of VEGF knockdown (%KD) are also shown. Values are presented as mean \pm SD of sample duplicates.

target's region is not the cause for the increased levels of VEGF-mRNA associated with MC-shRNA transfection. Additionally, the opposite effects indicate that the transcribed shRNA does not result in the theoretical siRNA molecule (identical to the synthetic siRNA) after processing. Thus, a problem involving the correct processing of the transcript might be causing the observed discrepancies. In fact, poly-adenylation coupled with Pol II transcription abolishes its ability to express RNA with clear-cut ends, originating long, undefined shRNAs molecules.³⁴ Therefore, pre-miRNA-like shRNAs driven by Pol II might not be recognized by Dicer, which is responsible for the processing of the shRNA into functional siRNA duplexes that will incorporate the RISC complex for target-specific mRNA degradation.^{15,16,34} Consequently, the transcribed shRNA might be acting as transcriptional activator of VEGF, as a consequence of off-target effects.¹⁸ As such, in order to test this hypothesis, a parental plasmid mimicking the expressing unit of pSilencer™ adeno 1.0-CMV System and encoding the same shRNA, was constructed as an attempt to originate a more defined shRNA transcript and straightforwardly processed – pshRNA_2. For that, the terminal sequence for the pshRNA CMV promoter was modified and the BGH polyadenylation signal was replaced by the synthetic polyA signal of the pSilencer™ adeno 1.0-CMV System (text-based sequence present at the manufacturer's website³⁵) (data not shown). The minicircle production and purification was performed as previously (data not shown).

Lipofection of BM-MSCs and MCF-7 with the new minicircle MC-shRNA_2

In order to evaluate the effect of the synthetic siRNA and MCs encoding a shRNA targeting VEGF (MC-shRNA and MC-shRNA_2) on MCF-7 cells, cells were transfected with the Lipofectamine reagent. The synthetic siRNA and MC-shRNA were used as controls. In this experiment, two different amounts of MC-shRNA/MC-shRNA_2 and synthetic siRNA were used to transfect MCF-7 cells, that were collected 48 hours post-transfection. Afterwards, the collected cells were used to quantify the VEGF-mRNA by

RT-qPCR using the $2^{-\Delta\Delta Ct}$ method (Figure 7). The results further confirm the silencing potential of the synthetic siRNA showed previously after BM-MSC transfection (Figure 6), reaching a knockdown of 49% at a concentration of 100nM (Figure 7).

It is possible to note that, despite the silence efficiency variability associated to the transfection of different cell types, the %KD obtained are relatively similar. Regarding the MC-shRNA transfection, the results support the previously obtained data since it leads to increased levels of VEGF-mRNA relatively to the control cells (MCF-7 LF). In addition, it is possible to note that higher amounts of MC lead to higher levels of VEGF-mRNA, reaching 5.4- and 6.3-fold when transfected with 500ng and 1000ng of MC-shRNA, respectively (Figure 7). Furthermore, the results of transfection with the new minicircle MC-shRNA_2, revealed that the effect of increased expression appears to be conserved; however, the up-regulation seems to be attenuated relatively to MC-shRNA, since a 1.5- and 1.8-fold increase was observed after transfection with 500ng and 1,000ng, respectively (Figure 7).

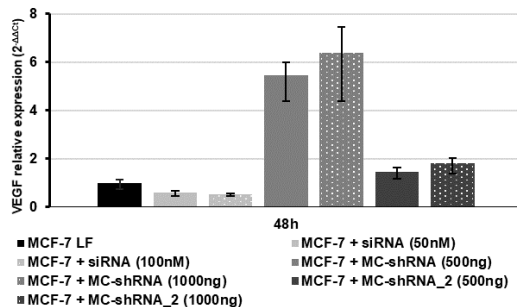


Figure 7- Evaluation of transgene delivery 48 hours after lipofection of MCF-7 with different amounts of MC-shRNA, MC-shRNA_2 or synthetic siRNA, by analysis of VEGF gene expression by RT-qPCR. The values were obtained using $2^{-\Delta\Delta Ct}$ method, with GAPDH as the endogenous control gene and MCF-7 transfected without pDNA/siRNA, as baseline. The percentages of VEGF knockdown (%KD) are also shown. Values are presented as mean \pm SD of sample duplicates.

To further validate the effect of the new minicircle MC-shRNA_2 on VEGF expression, BM-MSC were also transfected. Through the results in Figure 8, it is possible to verify that MC-shRNA_2 did not silence VEGF expression, since increased levels of VEGF-mRNA were

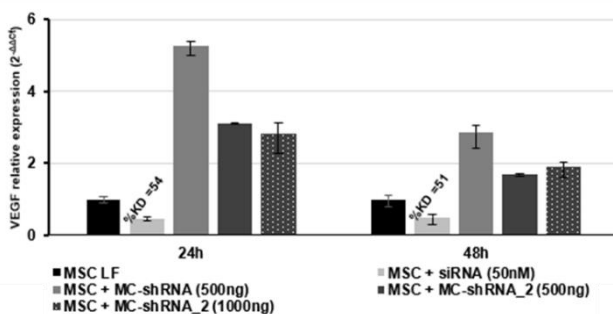


Figure 8- Evaluation of transgene delivery 24 and 48 hours after lipofection BM-MSC with MCs or synthetic siRNA, by analysis of VEGF gene expression by RT-qPCR. The values were obtained using $2^{-\Delta\Delta Ct}$ method, with GAPDH as the endogenous control gene and MSC transfected without pDNA/siRNA, collected after 24h and 48h, as baseline. The percentages of VEGF knockdown (%KD) are also shown. Values are presented as mean \pm SD of sample duplicates.

obtained compared to the control (MSC LF), both 24h and 48 h post transfection, as seen in MCF-7 cells transfection (Figure 7). Regarding synthetic siRNA transfection, the silencing effect appears to be stronger than before (Figure 6), exhibiting a knockdown of 54% and 51%, 24h and 48h post-transfection respectively (Figure 8). Overall, these experiments revealed that MC-shRNA_2 appears to induce a similar cellular response. As such, the modifications performed in the MC promoter and termination signal might not be enough to originate a well-defined pre-miRNA-like shRNA capable of being processed by Dicer. Therefore, a different promoter with a well-defined transcription initiation and termination, such as U6 promoter, could be a promising option to be tested in future studies.³⁴

ELISA quantification of VEGF secretion by transfected cells

To further validate the efficacy of siRNA/shRNA in silencing VEGF production and consequent secretion, a final VEGF quantification at the protein level was performed using an ELISA assay. For that, cell supernatants collected 48h after transfection of BM-MSC and MCF-7 with the synthetic siRNA or shRNA-expressing MCs were tested. Cell supernatants from cells transfected only with lipofectamine were used as controls and all samples were tested in duplicate. After normalization with the correspondent cell number and volume of the culture supernatant of the different conditions, the mass of VEGF produced was obtained (Figure 9).

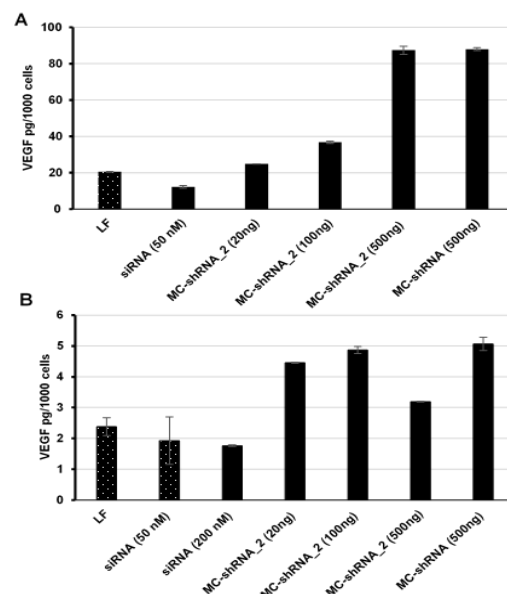


Figure 9- Evaluation of transgene delivery 48 hours after transfection of (A) BM-MSC and (B) MCF-7 with the synthetic siRNA, MC-shRNA or MC-shRNA_2, by analysis the VEGF protein production by ELISA. Cells transfected with LF were used as control and values are presented as mean \pm SD of sample duplicates (solid bar) or as mean values \pm SEM from two samples of independent experiments (dotted).

Through the analysis of the results from transfected BM-MSC (Figure 9A) it is possible to observe that cells transfected with the synthetic siRNA secrete lower

amounts of VEGF (12.3 ± 0.8 pg/1000 cells) relatively to the control (20.5 ± 0.2 pg/1000 cells) exhibiting a 40% decrease in protein production. This result is consistent to the ones obtained for VEGF expression at the mRNA level through RT-qPCR. On the other hand, cells transfected with shRNA-expressing MCs produced more VEGF than the control and that increase, as seen at the mRNA level, is proportional to the amount of MC transfected, reaching a ~4-fold increase in protein production when transfected with 500 ng of MC (approximately 88 pg/1000 cells). The basal levels of VEGF secreted by the control cells similar to the one reported in Serra *et al* (2018)³⁶ in which a VEGF production rate of 11.1 ± 3.4 pg/1000 cells.day was obtained for non-transfected BM-MSCs. Although the results are derived from a single experiment, leading to the need of further studies, similar tendencies in expression change were observed. Regarding the results from transfected MCF-7 (Figure 9B), it is possible to confirm that silencing efficacy of the siRNA is inferior, showing a maximum of 25% decrease in VEGF production relatively to the control. Once again, cells transfected with the MC induce VEGF production which is consistent with the increase levels of mRNA obtained in the RT-qPCR results. Interestingly, despite being a cancer cell line, it is possible to note that the overall levels of VEGF secreted by MCF-7 cells are approximately 10 times lower than BM-MSCs (2.38 pg/1000 cells vs 20.5 ± 0.2 pg/1000 cells).

Overall, the synthetic siRNA is able to silence VEGF expression leading to a decrease in protein production and consequent secretion. This result was expected, since this siRNA sequence was used in previous studies reporting a substantial decrease in VEGF protein levels.^{19,20} Regarding the MC-derived shRNA, it was possible to conclude that it induces the expression of VEGF, leading to increase levels of protein production and secretion, eliminating the hypothesis that the shRNA could be silencing VEGF by repressing translation instead of target cleavage/degradation.

Angiogenic capacity of the engineered BM-MSC and MCF-7 assessed by *in vitro* tube formation assay

Finally, within the scope of this thesis, it was performed an assay that relies on the capacity of human umbilical vein endothelial cells (HUVEC) to form tube networks when cultured in Matrigel to evaluate the angiogenic potential of the transfected cells – *in vitro* tube formation assay. For that, conditioned medium (CM) from transfected cells collected after 48h in culture, was used to cultivate HUVECs. The tube formation assay was accomplished using CM from BM-MSCs transfected with the synthetic siRNA and MC-shRNA_2 (Figure 10). CM from transfected MCF-7 were also tested (*data not shown*). CM from cells transfected only with lipofectamine were used as controls and all samples were tested in duplicate. Through the analysis of the results, it is possible to note that the CM retrieved from the culture of BM-MSC

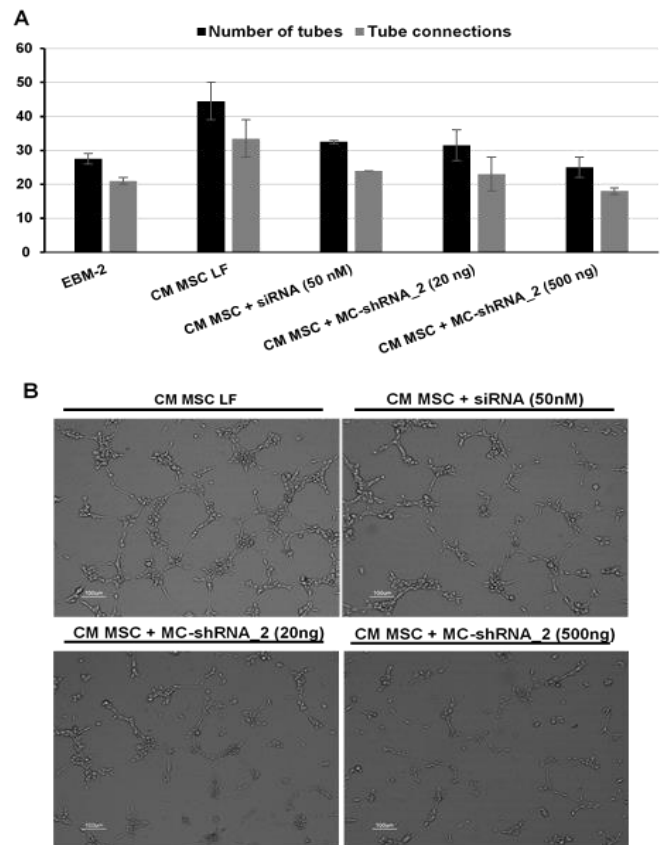


Figure 10- Tube formation assay results obtained for BM-MSCs conditioned medium after transfection with the synthetic siRNA and MC-shRNA_2. **(A)** Number of tubes and tube connections for each condition observed per optical field after 6 h in culture. Values are presented as mean \pm SD of sample duplicates. **(B)** Bright field images (100X) of HUVECs tube formation after 6h in culture with each condition of BM-MSC CM.

transfected with lipofectamine induced the formation of more tubes (44.5 ± 5.5) and connections (33.5 ± 5.5) to compared to the negative control basal medium EBM-2 (27.5 ± 1.5 and 21.0 ± 1.0 , respectively). Additionally, CM from cells transfected with the siRNA showed a decreased potential to induce tube formation, exhibiting the formation of 32.5 ± 0.5 tubes and 24.0 ± 0.0 branch points, suggesting a reduced angiogenic potential compared to control BM-MSC. These results were expected since the amount of VEGF in the CM determined by ELISA (*data not shown*) was lower in the case of the cells transfected with the siRNA. As such, lower VEGF levels would minimize HUVEC tube formation capacity due to its pro-angiogenic features. On the other hand, the tube formation results obtained for the CM retrieved from cells transfected with MC-shRNA_2 were not the expected ones, since they also showed a decreased potential to induce tube formation and the levels of VEGF were superior or at least similar to ones for BM-MSC lipofectamine control (*data not shown*). This result could be associated to the secretion of toxic elements to the CM after transfection with the MC, however this effect was not reported in previous studies³⁶ and further studies are required in order to validate it.

CONCLUSIONS AND FUTURE STUDIES

MSCs have an active role in supporting the maintenance of a dynamic and homeostatic tissue microenvironment by secretion of a broad range of biologically active molecules. Upon interaction with cancer cells, MSCs became active participants in tumour development namely by promoting angiogenesis through the secretion of pro-angiogenic molecules such as VEGF. Tumour angiogenesis is one of the hallmarks of cancer progression, thus tackling this phenomenon seems a plausible approach to slow down tumour growth. At the present work, the primary goal was to develop a siRNA-based system capable of blocking VEGF expression and secretion in BM-MSCs and also cancer cells, and consequently diminishing their pro-angiogenic potential. For that, a selected synthetic siRNA was used in the *in vitro* transfection MSCs and MCF-7 cells. Parallely, minicircle vectors encoding a shRNA, targeting the same location of VEGF-mRNA, were also constructed, produced and purified for further transfection. In order to evaluate VEGF silencing, VEGF-mRNA and VEGF-protein levels were quantified by RT-qPCR and ELISA, respectively. Finally, *in vitro* tube formation assays were used to evaluate the effect of VEGF silencing on the angiogenic potential of the transfected cells. Concerning siRNA transfection, it revealed to efficiently silence VEGF expression at the mRNA level, inducing a knockdown of approximately 50% and 40%, 48 hours post-transfection with a concentration of 50nM and Lipofectamine, in MSCs and MCF-7, respectively. The ELISA results indicate a decrease in VEGF production and secretion relatively to the control, exhibiting a 40% after BM-MSC transfection. Regarding the preliminary results of functional assays, the siRNA-mediated reduction of VEGF production from transfected cells appears to potentiate a decrease in HUVEC tube formation capacity, and therefore, a decrease their angiogenic potential. Nevertheless, further studies should be performed in order to optimize siRNA transfection, and consequently silencing efficiency, namely by testing different LF/siRNA ratios, since a fixed amount of LF was used throughout the work. Additionally, although out of the aim of this master thesis, alternative delivery systems, that could facilitate the transition into *in vivo* studies should be explored, such as MSC-derived exosomes, since increasing evidence has revealed that the mechanism of interaction between stem cells and tumour cells involves the exchange of biological material through exosomes.³⁷ Regarding the development of the shRNA-expression system, a minicircle vector was selected based on the high transfection efficiencies and lack of biosafety concerns reported. A first parental plasmid expressing a pre-miRNA-like shRNA, targeting the same region as the synthetic siRNA, was successfully constructed as designed. The production and purification methods previously developed in the iBB-BERG laboratory²⁹ were shown to successfully isolate the MC,

although problems associated with excess RNA leading to the chromatographic column overload and consequent incomplete MC isolation, should be addressed. The transfection experiments with the shRNA-expressing MC, revealed that, contrary to the expected increased VEGF-mRNA levels were obtained, exhibiting ~3-fold and ~5-fold higher mRNA copies of VEGF than the control cells, 48h after transfection with 500 ng of MC, in BM-MSC and MCF-7 respectively. The opposite effects between the transfection of the synthetic siRNA and shRNA-expressing MC indicate that the transcribed shRNA does not result in the theoretical siRNA molecule (identical to the synthetic siRNA) after processing. Thus, a problem involving the correct shRNA processing into functional siRNA duplexes might be causing the observed discrepancies. Since polyadenylation coupled with Pol II transcription (CMV promoter) abolishes its ability to express RNA with clear-cut ends, originating long, undefined shRNAs molecules possibly preventing Dicer recognition, and consequently the correct processing. As a result of this incorrect processing, the transcribed shRNA can be acting as transcriptional activator of VEGF, as a consequence of off-target effects. Considering this hypothesis, a second MC vector mimicking the expressing unit of a commercial viral vector, with a different CMV promoter sequence and alternative termination signal, was developed as an attempt to obtain a more defined transcription. However, transfection experiments showed that, although up-regulation seems to be attenuated, the effect of increased expression is conserved. Furthermore, the ELISA results indicate once more an increase in VEGF production and secretion in the conditions transfected with the two MCs relatively to the control. As such, the modifications performed in the MC promoter and termination signal could not be enough to originate a well-defined pre-miRNA-like shRNA capable of being processed by Dicer. In this regard, further experiments should focus on determining the final structure of the shRNA transcript, such as by microRNA-sequencing³⁸ or by Northern-blot using probes targeting the guide sequence the siRNA³⁹. Additionally, transfection experiment using an empty vector should be performed to discard the possibility that the vector is the cause of VEGF up-regulation. An alternative approach might be the development of a vector containing a Pol III promoter, such as U6 promoter, that will lead to a more defined and easier to process pre-miRNA-like shRNA, or by maintaining the Pol II promoter, developing a vector with the shRNA sequence adapted into a pri-miRNA-like structure that will be readily recognized and processed by Drosha-DGCR8 microprocessor, before Dicer processing.³⁴ In conclusion, this study provides insights regarding the implementation of an siRNA-based system that targets VEGF expression, aiming at slowing down tumour angiogenesis.

REFERENCES

1. Adair, T. H. & Montani, J.-P. *Angiogenesis*. *Angiogenesis* (Morgan & Claypool Life Sciences, 2010).
2. Salajegheh, A. Introduction to Angiogenesis in Normal Physiology, Disease and Malignancy. in *Angiogenesis in Health, Disease and Malignancy* 1–9 (Springer International Publishing, 2016). doi:10.1007/978-3-319-28140-7_1
3. Carmeliet, P. Angiogenesis in life, disease and medicine. *Nature* **438**, 932–936 (2005).
4. De Palma, M., Biziato, D. & Petrova, T. V. Microenvironmental regulation of tumour angiogenesis. *Nat. Rev. Cancer* **17**, 457–474 (2017).
5. Wang, Z. *et al.* Broad targeting of angiogenesis for cancer prevention and therapy. *Semin. Cancer Biol.* **35**, S224–S243 (2015).
6. Carmeliet, P. & Jain, R. K. Principles and mechanisms of vessel normalization for cancer and other angiogenic diseases. *Nat. Rev. Drug Discov.* **10**, 417–427 (2011).
7. da Silva Meirelles, L., Fontes, A. M., Covas, D. T. & Caplan, A. I. Mechanisms involved in the therapeutic properties of mesenchymal stem cells. *Cytokine Growth Factor Rev.* **20**, 419–427 (2009).
8. Caplan, A. I. & Correa, D. The MSC: an injury drugstore. *Cell Stem Cell* **9**, 11–5 (2011).
9. Pittenger, M. F. *et al.* Multilineage potential of adult human mesenchymal stem cells. *Science* **284**, 143–7 (1999).
10. Crisan, M. *et al.* A perivascular origin for mesenchymal stem cells in multiple human organs. *Cell Stem Cell* **3**, 301–13 (2008).
11. Chapel, A. *et al.* Mesenchymal stem cells home to injured tissues when co-infused with hematopoietic cells to treat a radiation-induced multi-organ failure syndrome. *J. Gene Med.* **5**, 1028–1038 (2003).
12. Lazennec, G. & Lam, P. Y. Recent discoveries concerning the tumor - mesenchymal stem cell interactions. *Biochim. Biophys. Acta - Rev. Cancer* **1866**, 290–299 (2016).
13. Ferrara, N., Gerber, H.-P. & LeCouter, J. The biology of VEGF and its receptors. *Nat. Med.* **9**, 669–676 (2003).
14. Hoeben, A. Vascular Endothelial Growth Factor and Angiogenesis. *Pharmacol. Rev.* **56**, 549–580 (2004).
15. Karagiannis, T. C. & El-Osta, A. RNA interference and potential therapeutic applications of short interfering RNAs. *Cancer Gene Ther.* **12**, 787–795 (2005).
16. Moore, C. B., Guthrie, E. H., Huang, M. T.-H. & Taxman, D. J. Short hairpin RNA (shRNA): design, delivery, and assessment of gene knockdown. *Methods Mol. Biol.* **629**, 141–58 (2010).
17. Ozcan, G., Ozpolat, B., Coleman, R. L., Sood, A. K. & Lopez-Berestein, G. Preclinical and clinical development of siRNA-based therapeutics. *Adv. Drug Deliv. Rev.* **87**, 108–119 (2015).
18. Wittrup, A. & Lieberman, J. Knocking down disease: a progress report on siRNA therapeutics. *Nat. Rev. Genet.* **16**, 543–552 (2015).
19. Zuo, L., Fan, Y., Wang, F., Gu, Q. & Xu, X. A siRNA targeting vascular endothelial growth factor-A inhibiting experimental corneal neovascularization. *Curr. Eye Res.* **35**, 375–384 (2010).
20. Feng, W. *et al.* siRNA-mediated knockdown of VEGF-A, VEGF-C and VEGFR-3 suppresses the growth and metastasis of mouse bladder carcinoma in vivo. *Exp. Ther. Med.* **1**, 899–904 (2010).
21. Eswarappa, S. M. *et al.* Programmed translational readthrough generates antiangiogenic VEGF-Ax. *Cell* **157**, 1605–1618 (2014).
22. Park, J. H., Hong, S. W., Yun, S., Lee, D. & Shin, C. Effect of siRNA with an Asymmetric RNA/dTdT Overhang on RNA Interference Activity. *Nucleic Acid Ther.* **24**, 364–371 (2014).
23. Moore, C. B., Guthrie, E. H., Huang, M. T. & Taxman, D. J. Short Hairpin RNA (shRNA): Design, Delivery, and Assessment of Gene Knockdown. *Methods Mol. Biol.* 1–15 (2013). doi:10.1007/978-1-60761-657-3
24. Brummelkamp, T. R. A System for Stable Expression of Short Interfering RNAs in Mammalian Cells. *Science (80-)*. **296**, 550–553 (2002).
25. Protocol for Annealing Oligonucleotides | Sigma-Aldrich. Available at: <https://www.sigmaaldrich.com/technical-documents/protocols/biology/annealing-oligos.html>. (Accessed: 13th January 2018)
26. Brito, L. *Minicircle production and delivery to human mesenchymal stem/stromal cells for angiogenesis stimulation*. (2014).
27. Michaela Simcikova. Development of a process for the production and purification of minicircles for biopharmaceutical applications. (Instituto Superior Técnico, Universidade de Lisboa, 2013).
28. Mayrhofer, P., Schleefer, M. & Jechlinger, W. Use of Minicircle Plasmids for Gene Therapy. in *Methods in molecular biology (Clifton, N.J.)* **542**, 87–104 (2009).
29. Silva-Santos, A. R., Alves, C. P. A., Prazeres, D. M. F. & Azevedo, A. M. A process for supercoiled plasmid DNA purification based on multimodal chromatography. *Sep. Purif. Technol.* **182**, 94–100 (2017).
30. Alves, C. P. A., Šimčíková, M., Brito, L., Monteiro, G. A. & Prazeres, D. M. F. Development of a nicking endonuclease-assisted method for the purification of minicircles. *J. Chromatogr. A* **1443**, 136–144 (2016).
31. Boura, J. S., Santos, F., Gimble, J. M., Cardoso, C. M. P. & Madeira, C. Direct Head-To-Head Comparison of Cationic Liposome-Mediated Gene Delivery to Mesenchymal. **48**, 38–48 (2013).
32. Thomas, C. E., Ehrhardt, A. & Kay, M. A. Progress and problems with the use of viral vectors for gene therapy. *Nat. Rev. Genet.* **4**, 346–358 (2003).
33. Gaspar, V. *et al.* Minicircle DNA vectors for gene therapy: advances and applications. *Expert Opin. Biol. Ther.* **15**, 353–379 (2015).
34. Bofill-De Ros, X. & Gu, S. Guidelines for the optimal design of miRNA-based shRNAs. *Methods* **103**, 157–166 (2016).
35. pSilencer adeno 1.0-CMV System: Shuttle Vector 1.0 CMV. *ThermoFisher Scientific* Available at: <https://www.thermofisher.com/pt/en/home/life-science/dna-rna-purification-analysis/napamisc/vector-maps/psilencer-adeno-1.html#vector>. (Accessed: 3rd October 2018)
36. Serra, J. *et al.* Engineering of human mesenchymal stem/stromal cells (MSC) with VEGF-encoding minicircles for angiogenic gene therapy. *Hum. Gene Ther.* hum.2018.154 (2018). doi:10.1089/hum.2018.154
37. Wu, J., Qu, Z., Fei, Z.-W., Wu, J.-H. & Jiang, C.-P. Role of stem cell-derived exosomes in cancer. *Oncol. Lett.* **13**, 2855–2866 (2017).
38. Tam, S., Tsao, M.-S. & McPherson, J. D. Optimization of miRNA-seq data preprocessing. *Brief. Bioinform.* **16**, 950–963 (2015).
39. Koscianska, E. *et al.* Northern blotting analysis of microRNAs, their precursors and RNA interference triggers. *BMC Mol. Biol.* **12**, 14 (2011).